

Analysis of stresses in Al-5%Si alloy under loading conditions

J. Borowiecka-Jamrozek, J. Lachowski

Kielce University of Technology, Al. Tysiąclecia PP 7, 25-314 Kielce, Poland

* Corresponding e-mail address: jamrozek@tu.kielce.pl, jlach@tu.kielce.pl

Received 13.05.2014; published in revised form 01.07.2014

ABSTRACT

Purpose: This paper analyses the structure and tensile strength of AlSi5Cu2 silumin produced in accordance with PN-EN 1706:2001, categorized as C355 in the US. The study was supplemented with a numerical failure analysis conducted with Abaqus 6.12.

Design/methodology/approach: The alloy selected for this study was an Al base alloy containing 5% Si and 2% Cu. Tensile tests on notched round bars with three sizes of the notch radius were performed.

Findings: A micromechanical model for the ductility of plastically deforming material was applied to the alloy using the finite-element program ABAQUS. The model is validated by comparing the predictions to experimental results.

Research limitations/implications: Average stress triaxiality and ductility for the three types of tensile test specimens were obtained.

Originality/value: This paper presented computer simulation of the stress state in notched specimens.

Keywords: Al-Si alloy; Tensile test; Voids; Computer modelling

Reference to this paper should be given in the following way:

J. Borowiecka-Jamrozek, J. Lachowski, Analysis of stresses in Al-5%Si alloy under loading conditions, Journal of Achievements in Materials and Manufacturing Engineering 65/1 (2014) 26-31.

ANALYSIS AND MODELLING

1. Introduction

Aluminium and its alloys found nowadays the broadest application in many type of engineering structures [1,2]. This paper analyses the structure and tensile strength of AlSi5Cu2 silumin containing 5% silicon and 2% copper by weight produced in accordance with PN-EN 1706:2001, categorized as C355 in the US [3]. The alloy was annealed during 3 h at temperature 500°C. The specimens for tensile testing were fabricated at the Foundry Research Institute in

Cracow. The study was supplemented with a numerical failure analysis conducted with Abaqus 6.12 [4].

2. Material and methods

The tensile tests were performed on standard smooth and U-notched specimens using an Instron universal testing machine. The tests were carried out at ambient temperature at a nominal strain rate of 3 mm/min. The U-notched pieces differed in radius (Fig. 1).

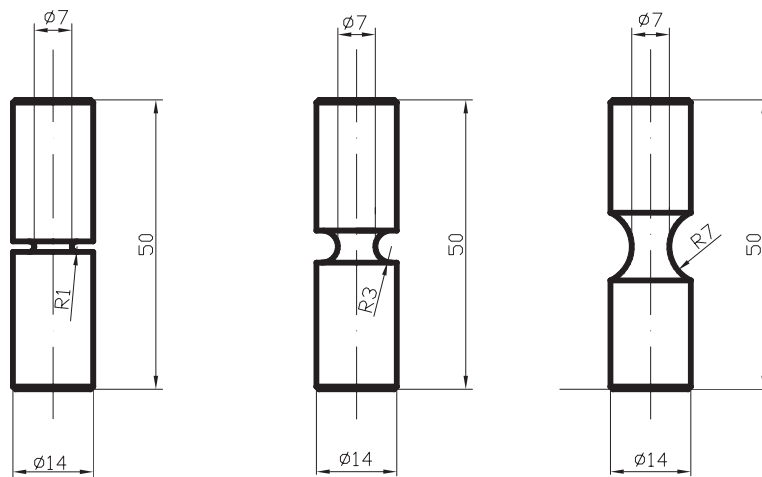


Fig. 1. U-notched specimens with a notch radius of 1 mm, 3 mm and 7 mm, respectively; all dimensions in mm

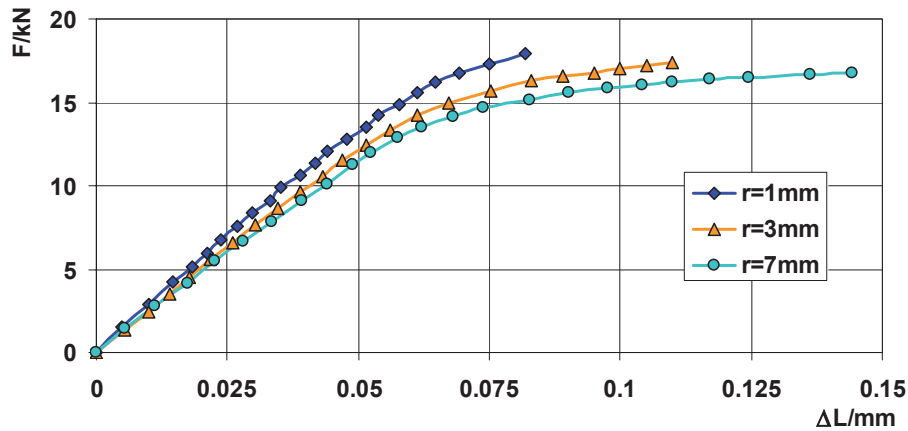


Fig. 2. Stress-strain curve for the notched specimens; relationship between tensile force F and elongation ΔL

First, a cylindrical specimen with a diameter of 4 mm and a gauge length of 25 mm was subjected to tension using an extensometer. The experimental data were used to calculate: the ultimate tensile strength ($R_m = 335$ MPa), the offset yield strength ($R_{0.2} = 280$ MPa), and the maximum elongation ($\Delta L/L = 3.5\%$). Then, tension was applied to three notched specimens with the notch radii $r = 1$ mm, 3 mm and 7 mm, respectively (Fig. 2).

The porosity of the material was determined by measuring its density using a hydrostatic balance. The initial porosity was reported to be about 2%. The initial diameter was measured before the test and the final diameter of the minimum cross-section was measured after fracture. The change in the diameter was used to calculate the mean elongation across the cross-section at fracture.

The material ductility was determined by applying the following formula:

$$\varepsilon_F = 2 \ln \left(\frac{d_I}{d_F} \right) \quad (1)$$

where d_I is the initial diameter of the specimen and d_F is the diameter of the minimum cross-section at failure. Table 1 shows the mean elongation at fracture. The structure of the material was analysed using a Jeol JSM 5400 scanning electron microscope equipped with an ISIS 300 X-ray spectrometer (Fig. 3). The chemical compositions of the silicon precipitates and the matrix are shown in Table 2. As can be seen from Fig. 3, the silicon particles are non-uniformly distributed in the structure and form clusters.

Table 1.
Maximum elongation in the neck

Notch radius	1 mm	3 mm	7 mm
$d_I - d_F$, mm	0.054 +/- 0.015	0.110 +/- 0.040	0.138 +/- 0.020
ε_F , %	1.61	3.17	3.98

Table 2.
Chemical compositions (%wt) of the Si precipitates and the matrix

Element	Al	Si	Cu
Silicon precipitate	3.50	96.50	
Matrix	95.34	1.01	2.28

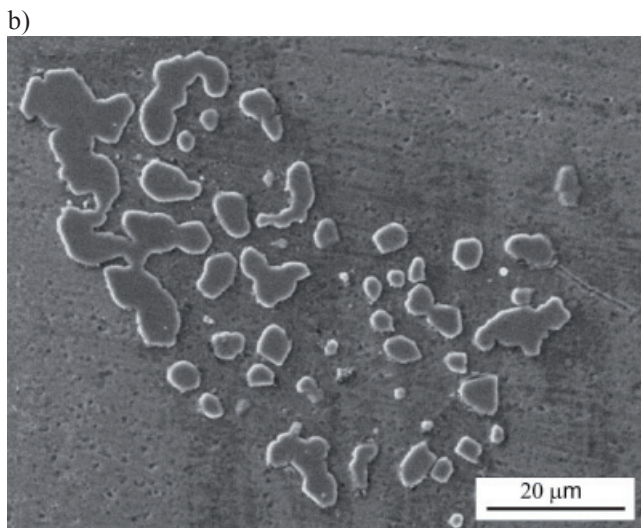
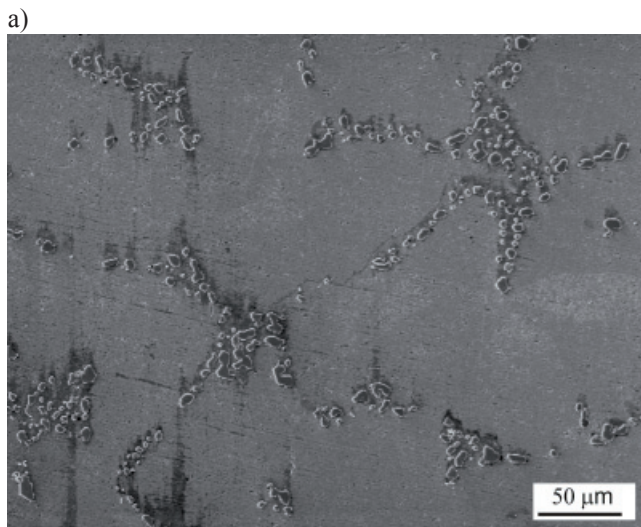


Fig. 3. Microstructure of the Al-5%Si alloy etched with 3% HF, a) magnification x 350, b) magnification x 1500

3. Analysis of stress at the notch cross-section

The parameter determining the spatial stress state is the stress triaxiality T [5], which is the ratio of the mean stress σ_m and the stress intensity σ_{red} determined with the Huber-Mises hypothesis. The stress triaxiality T for the plastically deforming alloy was calculated numerically using the Abaqus program. Figure 4 shows the numerically calculated the parameter T for different radii of the notch and across the whole cross-section of the specimen.

The stress triaxiality T was lower at the surface than in the centre. For small notch radii, the maximum was located away from the centre of the specimen. As shown in Fig. 5, the maximum elongation (1) in the neck decreases monotonically with an increase in the degree of stress triaxiality. When parameter T increased, the values of the maximum elongation for the alloys with a different content of Si were similar.

4. Computer simulation of the stress state in notched specimens

4.1. Model of plastic deformation of the material with voids

The Gurson-Tvergaard-Needleman constitutive equation (GTN model) for the material containing voids has the form [7-10]

$$\Phi = \frac{\sigma_{red}^2}{\sigma(\varepsilon)^2} + 2q_1 f^* \cosh\left(-q_2 \frac{3\sigma_m}{2\sigma(\varepsilon)}\right) - (1 + q_3 (f^*)^2) = 0 \quad (2)$$

where σ_{red} is the stress reduced according to the Huber-Mises hypothesis, σ_m is the mean stress, and $\sigma(\varepsilon)$ is the stress resulting from the actual stress-strain curve (Fig. 2). Coefficients q_i are the Tvergaard coefficients characterizing the plastic properties of a material. As there is no clear physical interpretation of these coefficients, in this study we assumed that $q_1 = q_2 = q_3 = 1$. The process of void coalescence during deformation is expressed by function f^* ,

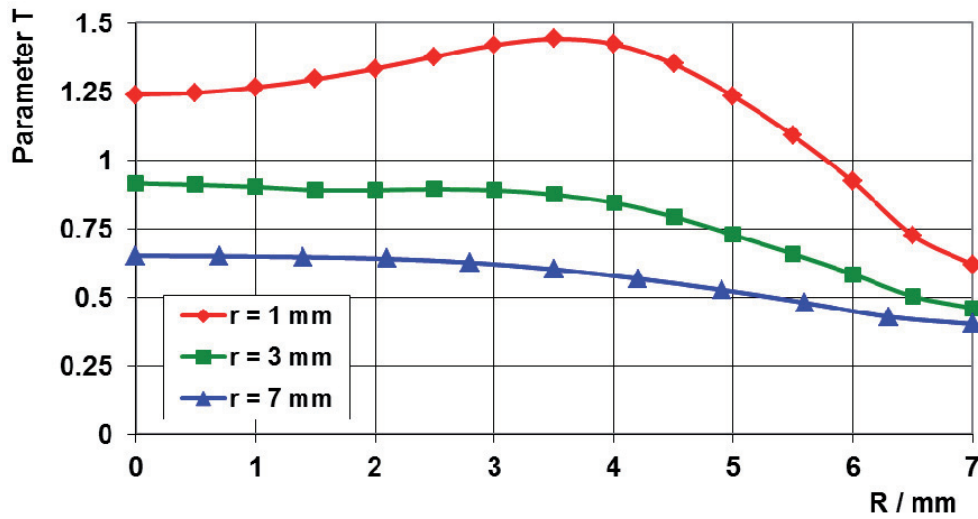


Fig. 4. Changes of stress triaxiality T in the specimen neck (R – distance from the centre of a specimen)

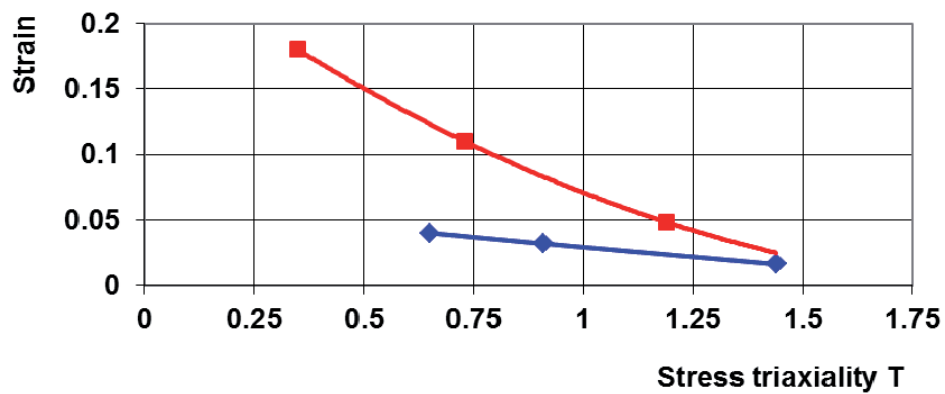


Fig. 5. Relationship between the maximum strain in the neck and the stress triaxiality T in the neck centre, red – relationship for Al-11%Si [6], blue – relationship for Al-5%Si

introduced by Tvergaard and Needleman [9,11]. Function f^* represents a rapid reduction in the transmitted load with increasing void volume fraction

$$f^*(f) = f \quad \text{for } f \leq f_c \quad (3a)$$

$$f^*(f) = f_c + \frac{1-f_c}{f_F-f_c}(f-f_c) \quad \text{for } f > f_c \quad (3b)$$

where f is the void volume fraction, f_c is the critical value of the void volume fraction above which the process of void nucleation occurs and the material strength drops rapidly. Parameter f_F is the void volume fraction at fracture. The critical void volume fraction f_c generally ranges from

0.04 to 0.12. [9,11,12]. The critical value of f_F is a material constant determined experimentally or numerically; it is assumed to be about 0.25 [8,9,12,13].

4.2. Nucleation and void growth

The model assumes that an increase in the void volume fraction f occurs as a result of the growth of voids present in the material and void formation on the Si particles (cracking and decohesion of the particles) with increasing plastic strains [4]

$$df = df_g + df_n \quad (4)$$

where df_g – is an increase in the number of voids present in the material, df_n – is an increase in the volume fraction of voids initiated during the deformation process. An increase in the voids present in the material results from the increase in plastic strains. In numerical modelling, the nucleation of new voids was determined using the following formula

$$df_n = A \cdot d\varepsilon^{pl} \quad (5)$$

where coefficient A represents the nucleation of voids in the form of normal distribution around a certain value of the mean strain [4,11]

$$A = \frac{f_N}{s_N \sqrt{2\pi}} \exp \left[-\frac{1}{2} \left(\frac{\varepsilon - \varepsilon_N}{s_N} \right)^2 \right] \quad (6)$$

where f_N represents the volume fraction of void nucleating particles, ε_N is the mean plastic strain at which nucleation occurs, and s_N is the standard deviation of nucleation.

5. Computer simulation results

The simulation conducted with Abaqus [4] using the GTN model (2) aimed at reconstructing the stress-strain curves for notched specimens. The theoretical stress-strain curves were compared with the experimental stress-strain curves taking into consideration the following parameters: initial volume fraction f_0 , volume fraction of void nucleating particles f_N , mean nucleation strain ε_N , standard deviation of nucleation s_N , critical void volume fraction f_C , and void volume fraction at fracture f_F . The best results were obtained for the values presented in Table 3.

Table 3.
Material parameters used in the computer simulation

f_0	f_N	ε_N	s_N	f_C	f_F
0.02	0.046	0.022	0.01	0.045	0.25

The matching of the theoretical curve to the experimental curve shows that the best fit was obtained for the specimen with a notch 1 mm in radius (Fig. 6a). In the case of the 3 mm notch, the computer simulation reconstruction of the experimental curve was approximate (Fig. 6b). For the specimen with a notch radius of 7 mm, the computer simulation failed to correctly represent the results of the tensile test.

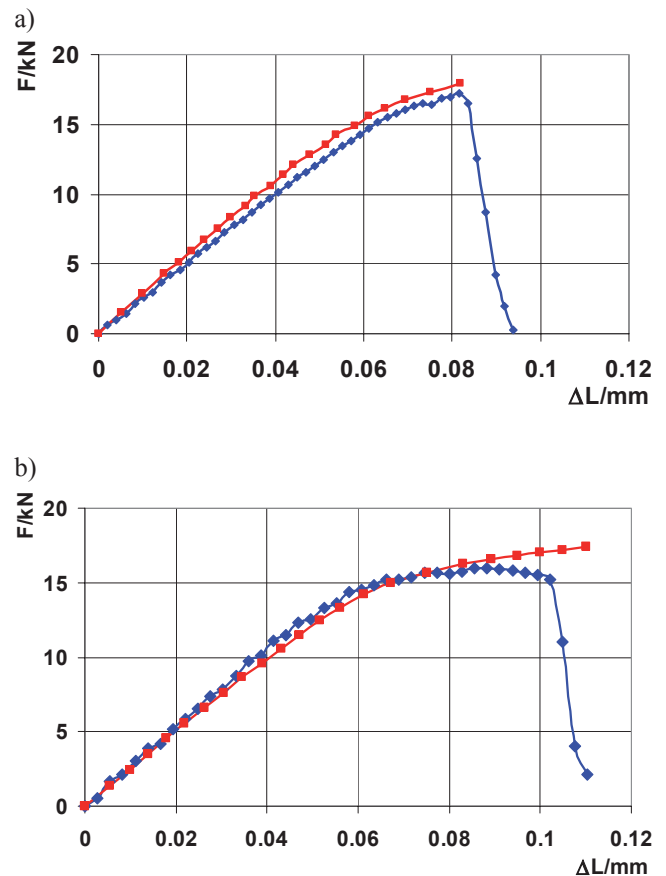


Fig. 6. Experimental curve (in red) vs computer-simulated curve (in blue) for the specimens with a notch of 1 mm – a), 3 mm – b)

6. Conclusions

The numerical analysis of the U-notched specimens showed large changes in both the Huber-Mises stress and the strain across the neck cross-section. The state of stress at failure at the minimum cross-section of the specimen cannot be determined from the outer diameter or the stress-strain curve. The GTN model for a material containing voids and precipitates on which voids form was used to explain the failure process at the spatial stress state. The model provides satisfactory simulation results for specimens with 1 mm and 3 mm notch radii. For specimens with a longer notch radius the fit of the curves was worse, which may indicate that failure was mainly due to tension, and this conclusion coincides with the Huber-Mises hypothesis.

Literature

- [1] A. Dziadoń, M. Drogosz, R. Mola, J. Borowiecka-Jamrozek, Laser Aging of Recasted Surface Layer of the Alloy AlSi5Cu2, *Ores and Non-ferrous Metals* 53/12 (2008) 795-799 (in Polish).
- [2] A. Dziadoń, J. Dudek, M. Konieczny, Influence of Laser Modification of Structure on Mechanical Properties of Al-Si Alloys, *Proceedings of the 3rd Pomeranian Science Conference "Materials Engineering 2002"*, Gdańsk-Wieżyca, 2002, 25-26 (in Polish).
- [3] M. Kutz (Ed.), *Handbook of Materials Selection*, John Wiley & Sons, 2002.
- [4] SIMULIA Dassault System, *Abaqus analysis user's manual*, Version 6.12, 2012.
- [5] G. Huber, Y. Brechet, T. Pardoen, Predictive model for void nucleation and void growth controlled ductility in quasi-eutectic cast aluminium alloys, *Acta Materialia* 53 (2005) 2739-2749.
- [6] A. Saigal, E.R. Fuller Jr., Analysis of Stresses in Al-5%Si Alloy Under Loading Conditions, *Computational Materials Science* 21 (2001) 149-158.
- [7] A.L. Gurson, Continuum theory of ductile rupture by void nucleation and growth, *Journal of Engineering Materials Technology* 99 (1977) 2-15.
- [8] V. Tvergaard, A. Needleman, Analysis of the cup-cone fracture in a round tensile bar, *Acta Metallurgica* 32/1 (1984) 157-169.
- [9] A. Needleman, V. Tvergaard, An analysis of ductile rupture in notched bars, *Journal of Mechanics and Physics of Solids* 32/6 (1984) 461-490.
- [10] P.G. Kossakowski, The prediction of ductile fracture to S235JR Steel using the stress modified critical strain and Gurson-Tvergaard-Needleman models, *Journal of Materials in Civil Engineering* 24 (2012) 1492-1500.
- [11] J. Koplik, A. Needleman, Void coalescence in porous plastic solids, *International Journal of Solids Structures* 24/8 (1988) 835-853.
- [12] A.B. Richelsen, V. Tvergaard, Dilatant plasticity or upper bound estimates for porous ductile solids, *Acta Metallurgica et Materialia* 42/8 (1994) 2561-2577.
- [13] A. Neimitz, A. Grzegorzcyk, Numerical analysis of the failure processes of plates made of S 960 QC steel, *Key Engineering Materials* 598 (2014) 184-189.